Mass Spectrometry

Observing the Hierarchical Self-Assembly and Architectural Bistability of Hybrid Molecular Metal Oxides Using Ion-Mobility Mass Spectrometry**

Johannes Thiel, Dongmei Yang, Mali H. Rosnes, Xiuli Liu, Carine Yvon, Stephanie E. Kelly, Yu-Fei Song,* De-Liang Long, and Leroy Cronin*

Polyoxometalates (POMs) are a class of anionic molecular metal oxide clusters existing between monomers and bulk infinite oxides based upon Mo, W, and V.[1] Although POM clusters can be well defined, there is a vast library of architectures varying in size and charge, and their assembly under far from equilibrium reaction conditions can even be compared to that of proteins in terms of primary, secondary, tertiary, and quaternary building blocks.[2,3] This is because the acidic condensation reactions of metal oxide polyhedra $[MO_x]$, leading to oligomeric $[MO_x]_n$ units (with $x = 4$ to 7), can be related to the assembly of the primary structure of a protein.[4] These building units are then able to undergo extended assembly processes, resulting in a variety of high nuclearity clusters that differ not only in terms of size and charge,[5] but also in shape and conformation, forming a range of supramolecular aggregates.[6]

This structural flexibility is tantalizing in terms of the potential for real design but, given the plethora of species in solution, understanding and hence controlling self-assembly is extremely demanding. In this respect we have recently been employing electrospray ionization mass spectrometry (ESI-MS) in the characterization of the primary, secondary, and tertiary structures of POM clusters.[7,8] Additionally, mechanistic studies revealed self-assembly processes involved at the secondary building block level.[9,10] Conventional MS allows for the separation of the anionic clusters by their mass and charge, that is, their *m/z* ratio, but the supramolecular quaternary structure, or isomers with the same size and charge, cannot be resolved by this method.[11] This is a major

limitation since the libraries of POM building blocks not only cover a wide range of masses and charges,[12] but they also show a high level of diversity by their size and conformational flexibility.[13]

Herein, we describe the use of ion-mobility mass spectrometry (IMS/MS),[14] recently used to examine protein structure and dynamics as well as some preliminary studies on coordination compounds,[15] as a new tool to probe metal oxide systems, allowing size separation and investigation of supramolecular assemblies as well as the conformation or folding of the cluster architectures. We are also able to show how the conformation of the clusters can be probed directly by engineering photoswitchable polyoxometalate hybrids that switch their conformation thereby changing their cross-sectional areas. To achieve these goals we chose to examine polymolecular aggregations of organic–inorganic hybrid Mn-Anderson clusters, $[MnMo_6O_{18}((OCH_2)_3CR)_2]^{3-}$ (Scheme 1),
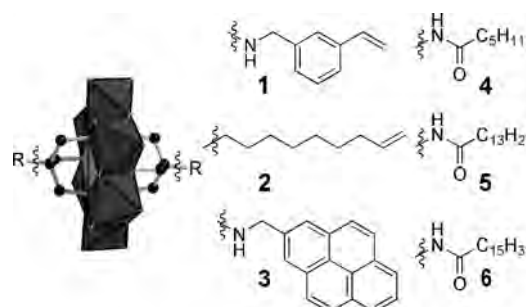
Scheme 1. Crystal structure of Mn-Anderson cluster $[MnMo_6O_{18}-((OCH_2)_3C-R)_2]^{3-}$ with MoO_6 octahedra in dark gray and the central MnO_6 octahedron in light gray. Carbon atoms are depicted as black spheres and the residues R for compounds **1** to **6** are drawn as skeletal formulae.[20]

and show the conformational change of photoswitchable molecules using IMS/MS. The Anderson clusters were chosen as model compounds for the primary investigative studies since they are a well-characterized class of compounds.[16] Also, the organo-derivatives of these clusters represent a well-defined library allowing the physical or chemical properties of the hybrid to be influenced by choice of the tethered organic group.[17,18] This means, by using the $\{MnMo_6O_{18}\}$ as the core, easy derivatization allows a wide diversity of hybrid cluster-organic complexes with respect to their overall charge, mass, size, and shape.[13,19]

[*] D. Yang, X. Liu, Dr. Y.-F. Song
State Key Laboratory of Chemical Resource Engineering
Beijing University of Chemical Technology, Beijing 100029 (China)
E-mail: songyufei@hotmail.com

Dr. J. Thiel, M. H. Rosnes, C. Yvon, S. E. Kelly, Dr. D.-L. Long,
Prof. L. Cronin
WestCHEM, Department of Chemistry
The University of Glasgow, Glasgow G12 8QQ (UK)
E-mail: l.cronin@chem.gla.ac.uk
Homepage: http://www.croninlab.com

© 2011 Wiley-VCH Verlag GmbH & Co. KGaA, Weinheim

Communications

The IMS/MS studies were performed on an ion-mobility mass spectrometer that combines travelling wave IMS (TWIMS) with a quadrupole/time-of-flight (Q/ToF) mass spectrometer. Six differently substituted Mn-Anderson clusters (Scheme 1) were investigated in both positive-ion and negative-ion mode, in the m/z range between 500 Da and 5000 Da. To perform these experiments, single crystals of compounds **1** to **6** were dissolved in acetonitrile and transferred to the gas phase by ESI. The IMS/MS spectrum analysis of compound **1** will be described herein in detail as an example, since this compound has a high affinity to form supramolecular assemblies in negative-ion mode. Additionally, the photoswitching of symmetric Mn-Anderson compounds substituted with azobenzene ligands, compounds **7**, **8**, and **9** results in a conformational shape change and we demonstrate how the two different conformers of each compound can be identified and characterized using the IMS/MS technique.

MS experiments of compounds **1** to **6**, without the use of ion-mobility separation, show complex overlapping envelopes of species which indicate the presence of supramolecular assemblies, possessing different charge states but the same m/z ratio. To deconvolute these envelopes, IMS was performed for the size separation of the polymolecular aggregations, allowing for the assignment of their overall composition (Figure 1).

Figure 1 shows a 2D spectrum of compound **1** where the x axis shows the m/z range and the y axis shows the drift time; the peak intensity is displayed according to a color code on a
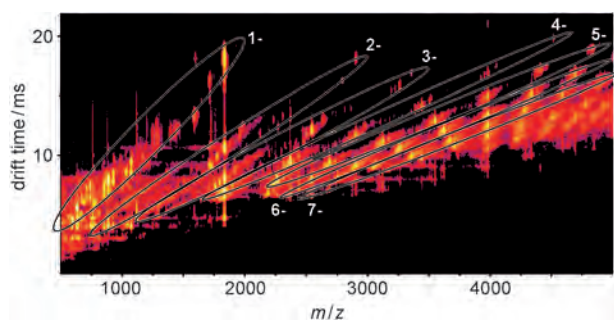

Figure 1. 2D IMS/MS spectrum of compound **1**. The diagonal lines of similarly charged species are encircled by ellipsoids and the charges of these species are given in white. (Background noise is filtered out for clarity; the original spectrum can be found in the Supporting Information.)

logarithmic scale.[14] To determine the compositions of identified peaks a combination of mass and drift time, that is, size fitting, was employed. First, this required analyzing the spectra to determine the formulae and the charges of the easily identifiable peaks. High intensity and sufficient resolution are crucial to identify the charge and hence the number of clusters and tetra-n-butylammonium (TBA) counterions that constitute the assembly represented in the peak envelope. A good starting point is the main peak consisting of one cluster plus two TBA cations and a charge of minus one, as well as multiples of that. For compound **1**, the peak envelope

around $m/z = 1872$ Da has been assigned as $[(\mathbf{1})\mathrm{TBA}_2]^-$ and has been separated into five peaks with the formula $\{[(\mathbf{1})\mathrm{TBA}_2]^-\}_n$ (with $n = 1, 2, 3, 4, 5$; see Figure 2). After deconvolution of a number of envelopes, the diagonal lines of
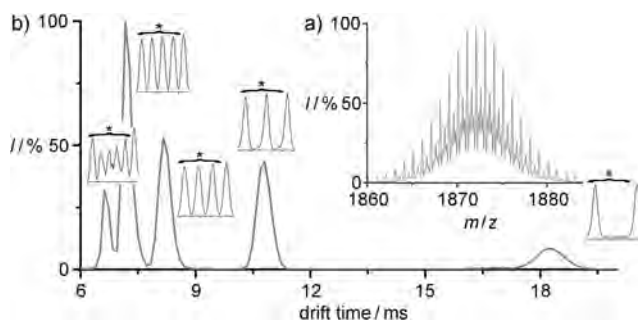

Figure 2. a) The mass spectrum for compound **1** for m/z 1860–1885 Da. b) The IM chromatogram for the deconvoluted peak envelope shown. The signals from left to right represent $\{[(\mathbf{1})\mathrm{TBA}_2]^-\}_n$ procession from $n = 5$ to $n = 1$, with frames of the time-resolved mass spectrum for charge determination. Asterisk marks 1 amu.

the peak envelopes with the same charge can be identified (Figure 1). Extrapolation of the trajectories defined by these lines towards higher m/z ratios, where resolution of the envelopes becomes insufficient, and taking neighboring lines into account, a determination of nearly all the peak assemblies was made.[14] This was confirmed by comparing the calculated cross-sections to the amount of clusters and TBAs assigned to the peaks.

All of the spectra were recorded under identical conditions for ease of comparison. In positive-ion as well as in negative-ion mode, compounds **1–6** have shown to form quaternary structures consisting of several clusters and TBA counterions. In general, compounds **1**, **2**, and **3** show a much higher tendency for aggregation than compounds **4**, **5**, and **6**. A full list of identified peaks is provided in the Supporting Information. When forming cationic assemblies in the MS, all Mn-Anderson clusters act in a similar fashion. One striking feature is that they tend to exchange TBA cations for protons, and occasionally, sodium cations, during the ionization process. The studies showed that the compounds can form assemblies of up to six clusters and 22 TBA cations resulting in $[(\mathbf{X})_6\mathrm{TBA}_{22}]^{4+}$ and nearly any smaller assembly that results in a maximum charge of $+4$. Even larger supramolecular assemblies with higher charges might be possible, but we decided to limit our experiments to the m/z range up to 5000 Da, as obtaining sufficient intensity becomes difficult at higher mass values.

The IMS/MS-spectra in negative-ion mode are somewhat more complex with much larger quaternary structures and even higher charge states. Assignments of these supramolecular assemblies tend to be difficult with resolution and intensity being relatively low. Only peak envelopes of sufficient intensity that have been clearly assigned using the aforementioned procedure will be considered for further discussion. The highest assembly was found for compound **3**, consisting of 20 clusters and 51 TBA cations, resulting in a charge of -9: $[(\mathbf{3})_{20}\mathrm{TBA}_{51}]^{9-}$. It is also the only investigated system where such a high charge has been observed for the

quaternary structure. Compounds **1** and **2** have also shown large assemblies with up to 17 clusters and 43 counterions: $[(\mathbf{1})_{17}TBA_{43}]^{8-}$ and $[(\mathbf{2})_{17}TBA_{43}]^{8-}$. The tendency to form larger aggregates is not very high for the Mn-Anderson cluster with long aliphatic chains (**4**, **5**, and **6**). While compounds **5** and **6** can arrange in configurations with a charge down to -6: $[(\mathbf{6})_{10}TBA_{24}]^{6-}$ and $[(\mathbf{5})_{12}TBA_{30}]^{6-}$, the lowest charge found for compound **4** is -5 with $[(\mathbf{4})_6TBA_{13}]^{5-}$. This shows that the tendency for the formation of quaternary structures is highly dependent on the length and type of ligand at the molecular level, that is, in the tertiary structure. The strong electrostatic forces between clusters and counterions govern the formation of the assemblies, but with those compounds with more extended π systems, it seems that the π–π interactions between ligands contribute considerably to the overall stability and determine the maximal size of the arrangements. Furthermore, preliminary studies using more polar solvents appeared to result in the transmission of smaller aggregates, and this is consistent with our previous work on the formation of supramolecular architectures in nonpolar solvents.[21,22]

To show the conformational change of a POM using IMS/MS, photoresponsive ligands in conjunction with the Mn-Anderson cluster have been used (compounds **7**, **8**, and **9**). These ligands consisted of two phenyl units bridged by an azo bond, which can either be in *trans* or *cis* conformation. One phenyl ring was attached to the cluster while the other unit carried alkoxo groups of different sizes (Scheme 2). Upon UV
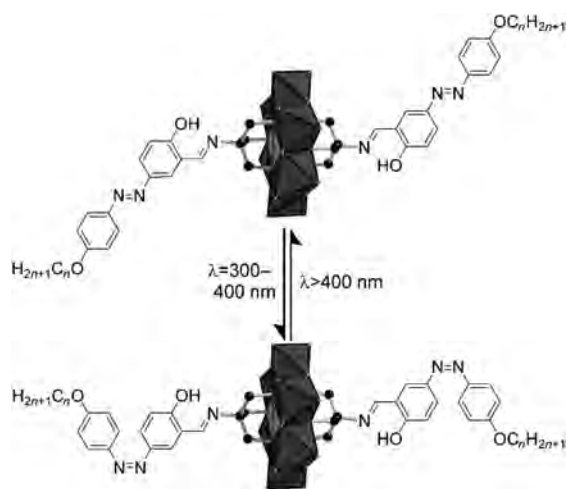
Scheme 2. Switching of photoresponsive Mn-Anderson cluster. Upon UV irradiation, the azo bond switches from *trans* to *cis* conformation. Under light irradiation, the bond switches back again. Three compounds (**7**, **8**, and **9** with $n = 8$, 10, and 12) where investigated.

irradiation at 365 nm for about 30 minutes, a conformational change of the azo bond from *trans* to *cis* occurred. If the sample was exposed to visible light for about 30 minutes, the process was reversed, resulting in the native *trans* conformation (Scheme 2). This process was repeated three times and was followed by IMS/MS and UV/Vis spectroscopy (see the Supporting Information). To prevent the reverse reaction as much as possible, the samples were handled under exclusion

of light, and IMS/MS measurements were conducted within 5 minutes after UV irradiation.

IMS/MS has been employed to follow the conformational change. Surprisingly, it has not been possible to observe peak envelopes for assemblies of only one Mn-Anderson cluster with two TBA cations. Applying the same conditions that were utilized for compounds **1** to **6**, only quaternary structures of two clusters and four TBA cations or more were found for compounds **7–9**. This indicates a very high interaction between the molecules, which is most likely due to strong π–π interactions between the ligands.

The conformational change itself resulted in a significant difference in the collision cross-section of the dimeric compounds, ranging from 13 Å^2 for the largest compound to 26 Å^2 for the ligand with the shortest aliphatic chain (Scheme 3). This fact manifests itself in the drift time spectra for the main peaks of the azo compounds (see Figure 3 and also the Supporting Information) where the equilibria for the formation of quaternary structures have clearly shifted. Figure 3 shows the drift time spectra for compound **7** in the m/z range of 2305–2320 Da before and after UV irradiation.

While the native compound (blue spectrum) exhibits only low intensity for the peak of a dimeric assembly centered around a drift time of 15.33 ms, the compound after UV irradiation shows a high intensity peak at 14.22 ms. This
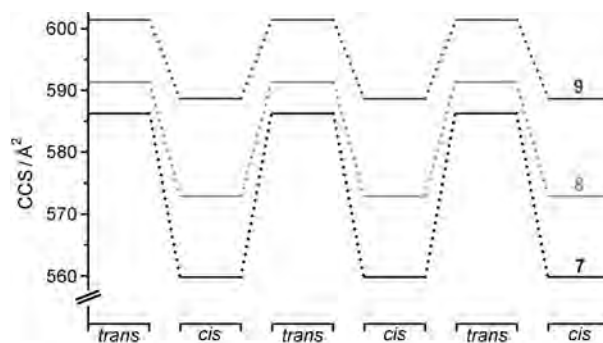
Scheme 3. Change in collision cross-section of dimers of compounds **7**, **8**, and **9** when switching between the *trans* and the *cis* conformation of the azo bond. The formula of the dimeric assemblies is $[(\mathbf{X})_2TBA_4]^{2-}$.
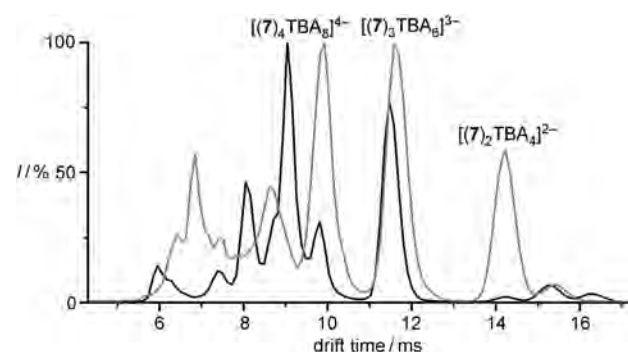

Figure 3. Comparison of the drift time graphs of the main envelope ($m/z = 2305$–2320 Da) for the native compound **7** (black) and after UV irradiation (gray). The spectra were consistent for all three repeated cycles.

indicates a higher stability of the two-cluster assembly in *cis* conformation compared to that with a *trans* conformation. The spectra after UV and after visible light irradiation were consistent through all three repetitions of the isomerization cycle for compounds **7**, **8**, and **9**, showing the reproducibility of this result.

In conclusion, we have shown how IMS/MS can be used to investigate polyoxometalates with the ability to form extraordinarily large aggregates. Although the link between solution chemistry and gas phase has yet to be established, the strong ligand interactions indicated by the supramolecular assemblies found in the IMS/MS measurements give strong indications for future studies in surface chemistry[11] and vesicle formation.[21,22] Furthermore, we have shown that clusters with photoswitchable conformations can be separated and investigated unambiguously for the first time upon transmission into the mass spectrometer. Such investigations have potential for aiding in the design of new cluster systems, including photoswitchable POM materials,[13] as well as elucidating the composition of new or unknown cluster systems, for example, the recently discovered uranyl peroxide cluster systems.[23] Finally, ion-mobility mass spectrometry opens up a crucial new dimension allowing the characterization of clusters according to both their size and charge, and therefore their charge density. This means this technique can be applied to cluster libraries, as well as investigating the supramolecular chemistry and structures of the clusters in solution and the gas phase.

Experimental Section

1: A mixture of $[N(n\text{-}C_4H_9)_4]_4[\alpha\text{-}Mo_8O_{26}]$ (2.2 g, 1.0 mmol), Mn-(OAc)$_3$·2H$_2$O (0.39 g, 1.5 mmol), vinylbenzyl-TRIS (0.80 g, 3.4 mmol; TRIS = tris(hydroxymethyl)aminomethane in acetonitrile (50 mL) was prepared and heated to reflux for 16 h. The orange/brown reaction mixture was then cooled down to room temperature and the precipitate was removed by centrifugation. To obtain single crystals, the solution was left undisturbed under diffusion of diethyl ether. Orange crystals were isolated after 3 days. Yield: 1.77 g (0.84 mmol, 63% based on Mo). Elemental analysis for $C_{74}H_{140}MnMo_6N_5O_{24}$ ($M_r = 2125.36$): C 42.03, H 6.67, N 3.31; found: C 41.88, H 6.67, N 3.35. ^{1}H NMR (CD$_3$CN, 400 MHz:) $\delta = 62.63$ (s, br, CH$_2$), 7.56 (s, 2H), 7.32 (m, 6H), 6.75 (m, 2H), 5.80 (d, 2H, $J = 17.6$ Hz), 5.22 (d, 2H, $J = 10.7$ Hz), 3.16 (m, 28H), 1.61 (s, 24H), 1.36 (s, 24H), 0.97 ppm (m, 36H); ^{13}C NMR (CD$_3$CN, 100 MHz): $\delta = 146.8$, 138.6, 137.9, 129.5, 129.3, 127.4, 125.4, 114.2, 59.3, 24.4, 20.7, 14.1 ppm. FTIR (KBr): $\tilde{v} = 2939.61$, 2870.17, 1481.38, 1381.08, 1149.61, 1064.74, 1033.88, 918.15, 802.41, 648.10 cm^{-1}.

5: $[N(n\text{-}C_4H_9)_4]_4[\alpha\text{-}Mo_8O_{26}]$ (1.02 g, 0.47 mmol), Mn(OAc)$_3$·2H$_2$O (0.20 g, 0.71 mmol), and myristic-TRIS (0.58 g, 1.6 mmol) were added to a solution MeCN (30 mL). The reaction heated to reflux for about 18 h. The reaction mixture was then cooled down to room temperature before the precipitate was removed by centrifugation. The mother liquid was set up for crystallization with diethyl ether diffusion. Orange crystals were isolated after 3 days. Yield: 0.82 g (0.35 mmol, 75% based on Mo). Elemental analysis for $C_{84}H_{176}Mn_1Mo_6N_5O_{26}$ ($M_r = 2313.63$): C 43.81, H 7.70, N 3.04; found: C 42.34, H 7.44, N 3.7. ^{1}H NMR (CD$_3$CN, 400 MHz): $\delta = 6.20$ (s, 2H), 3.10 (t, 24H, $J = 8.16$ Hz), 2.35 (s, 4H), 1.61 (m, 24H), 1.50 (s, 4H), 1.36 (q, 24H, $J = 7.1$ Hz), 1.27 (s, 40H), 0.97 (t, 36H, $J = 7.3$ Hz), 0.87 ppm (t, 6H, $J = 6.9$ Hz); ^{13}C NMR (CD$_3$CN, 100 MHz): $\delta = 175.21$, 59.31, 35.75, 32.66, 30.47, 30.42, 30.39, 30.33, 30.22, 30.16, 30.09, 27.17, 24.44, 23.41, 20.58, 14.43, 14.03 ppm. FTIR (KBr): $\tilde{v} =$

3302, 3210, 2924, 2855, 1736, 1667, 1543, 1466, 1381, 1381, 1250, 1103, 1026, 918, 802, 656 cm^{-1}.

7: A mixture of 5-(4-octyloxy-phenylazo)-benzaldehyde (**7a**) (0.7 g, 2.0 mmol) and TRIS-Mn-Anderson cluster with the molecular formula of $[N(n\text{-}C_4H_9)_4][MnMo_6O_{18}\{(OCH_2)_3CNH_2\}_2]$ (1.88 g, 1.0 mmol) in ethanol (60 mL) was heated to reflux for 6 h. The solvent was evaporated under reduced pressure, resulting in the formation of an orange product, which was further purified by recrystallization from EtOH/MeCN (1:1). Yield: 1.28 g (0.50 mmol, 50%). Elemental analysis for $C_{98}H_{172}MnMo_6N_9O_{28}$ ($M_r = 2555.04$): C 46.07, H 6.79, N 4.93; found: C 46.32, H 6.43, N 5.02. ^{1}H NMR (CDCl$_3$): $\delta = 0.89$ (s, 36H), 0.95 (s, 6H), 1.27 (m, 20H), 1.43 (m, 24H), 1.62 (m, 24H), 1.81 (m, 4H), 3.24 (s, 24H), 4.02 (s, 4H), 6.98 (d, 2H, $J = 7.2$ Hz), 7.10 (d, 1H, $J = 6.0$ Hz), 7.66 (s, 2H), 7.88 ppm (d, 2H, $J = 6.0$ Hz). ^{13}C NMR (CDCl$_3$): $\delta = 14.13$, 14.56, 20.91, 22.66, 24.07, 26.03, 29.46, 31.81, 58.57, 68.35, 114.69, 116.66, 124.42, 124.65, 127.05, 129.62, 144.07, 146.81, 161.18, 166.17 ppm. FTIR (KBr): $\tilde{v} = 3433$, 2961, 2927, 2871, 1623, 1599, 1482, 1382, 1284, 1251, 1149, 1102, 1035, 942, 921, 905, 841, 666, 563, 464 cm^{-1}.

Compounds **8** and **9** were synthesized in a similar way to that of **7** by reaction of 5-(4-decyloxy-phenylazo)-2-hydroxybenzaldehyde or 5-(4-Dodecyloxy-phenylazo)-2-hydroxybenzaldehyde and TRIS-Mn-Anderson in EtOH for 6 h. The resulting product **8** or **9** was obtained by recrystallization of the corresponding orange products from EtOH/MeCN (1:1). For compound **8**: Yield: 1.70 g (0.65 mmol, 65%). Elemental analysis for $C_{102}H_{180}MnMo_6N_9O_{28}$ ($M_r = 2611.14$): C 46.92, H 6.95, N 4.83; found C 46.68, H 6.61, N 4.98. ^{1}H NMR (d-CDCl$_3$): $\delta = 0.88$ (s, 36H), 0.96 (s, 6H), 1.28 (m, 28H), 1.44 (m, 24H), 1.63 (m, 24H), 1.81 (m, 4H), 3.26 (s, 24H), 4.03 (s, 4H), 7.00 (d, 2H, $J = 7.2$ Hz), 7.12 (d, 1H, $J = 6.0$ Hz), 7.66 (s, 2H), 7.89 (d, 2H, $J = 6.6$ Hz). ^{13}C NMR (CDCl$_3$, ppm): 14.13, 14.55, 20.93, 22.68, 24.08, 26.03, 29.40, 31.89, 58.57, 68.36, 114.69, 116.46 ≈ 116.66, 124.42, 127.04, 129.61, 144.08, 146.83, 161.18, 166.20 ppm. FT-IR (KBr): $\tilde{v} = 3438$, 2961, 2928, 2872, 1623, 1600, 1482, 1383, 1283, 1250, 1149, 1102, 1034, 942, 922, 904, 841, 668, 564, 468 cm^{-1}. For compound **9**: Yield: 1.65 g (0.62 mmol, 62%). Elemental analysis for $C_{106}H_{188}MnMo_6N_9O_{28}$ (2667.25): C 47.73, H 7.10, N 4.73; found: C 47.46, H 7.42, N 4.38. ^{1}H NMR (CDCl$_3$): $\delta = 0.88$ (t, 6H, $J = 13.8$ Hz), 0.97 (s, 36H), 1.32 (m, 36H), 1.45 (m, 24H), 1.64 (m, 24H), 1.82 (m, 4H), 3.26 (s, 24H), 4.03 (t, 4H, $J = 12.6$ Hz), 7.00 (d, 2H, $J = 8.4$ Hz), 7.13 (d, 1H, $J = 8.4$ Hz), 7.67 (d, 2H, $J = 7.8$ Hz), 7.89 ppm (d, 2H, $J = 8.4$ Hz). ^{13}C NMR (CDCl$_3$): $\delta = 14.13$, 14.46, 20.85, 22.69, 24.11, 26.03, 29.44, 31.92, 58.68, 68.33, 114.67, 116.65, 124.40, 126.98, 129.69, 144.09, 146.87, 161.14, 166.20 ppm. FTIR (KBr): $\tilde{v} = 3441$, 2960, 2928, 2871, 1623, 1599, 1482, 1382, 1283, 1251, 1150, 1103, 1034, 942, 921, 904, 840, 668, 564, 464 cm^{-1}.

[1] D. L. Long, R. Tsunashima, L. Cronin, *Angew. Chem.* **2010**, *122*, 1780–1803; *Angew. Chem. Int. Ed.* **2010**, *49*, 1736–1758.

[2] A. Müller, S. Sarkar, S. Q. N. Shah, H. Bögge, M. Schmidtmann, S. Sarkar, P. Kögerler, B. Hauptfleisch, A. X. Trautwein, V. Schünemann, *Angew. Chem.* **1999**, *111*, 3435–3439; *Angew. Chem. Int. Ed.* **1999**, *38*, 3238–3241.

[3] A. Müller, S. Roy, *Coord. Chem. Rev.* **2003**, *245*, 153–166.

[4] L. C. W. Baker, D. C. Glick, *Chem. Rev.* **1998**, *98*, 3–49.

[5] C. P. Pradeep, D. L. Long, G. N. Newton, Y. F. Song, L. Cronin, *Angew. Chem.* **2008**, *120*, 4460–4463; *Angew. Chem. Int. Ed.* **2008**, *47*, 4388–4391.

[6] M. L. Kistler, A. Bhatt, G. Liu, D. Casa, T. Liu, *J. Am. Chem. Soc.* **2007**, *129*, 6453–6460.

[7] Y. F. Song, D. L. Long, S. E. Kelly, L. Cronin, *Inorg. Chem.* **2008**, *47*, 9137–9139.

[8] M. Bonchio, O. Bortolini, V. Conte, A. Sartorel, *Eur. J. Inorg. Chem.* **2003**, 699–704.

[9] D. K. Walanda, R. C. Burns, G. A. Lawrance, E. I. von Nagy-Felsobuki, *J. Chem. Soc. Dalton Trans.* **1999**, 311–321.

[10] E. F. Wilson, H. N. Miras, M. H. Rosnes, L. Cronin, *Angew. Chem.* **2011**, *123*, 3804–3808; *Angew. Chem. Int. Ed.* **2011**, *50*, 3720–3724.

[11] M. H. Rosnes, C. Musumeci, C. P. Pradeep, J. S. Mathieson, D. L. Long, Y. F. Song, B. Pignataro, R. Cogdell, L. Cronin, *J. Am. Chem. Soc.* **2010**, *132*, 15490–15492.

[12] D. L. Long, E. Burkholder, L. Cronin, *Chem. Soc. Rev.* **2007**, *36*, 105–121.

[13] Y. Yan, H. B. Wang, B. Li, G. F. Hou, Z. D. Yin, L. X. Wu, V. W. W. Yam, *Angew. Chem.* **2010**, *122*, 9419–9422; *Angew. Chem. Int. Ed.* **2010**, *49*, 9233–9236.

[14] a) D. P. Smith, T. W. Knapman, I. Campuzano, R. W. Malham, J. T. Berryman, S. E. Radford, A. E. Ashcroft, *Eur. J. Mass Spectrom.* **2009**, *15*, 113–130; b) A. B. Kanu, P. Dwivedi, M. Tam, L. Matz, H. H. Hill, *J. Mass Spectrom.* **2008**, *43*, 1–22.

[15] E. R. Brocker, S. E. Anderson, B. H. Northrop, P. J. Stang, M. T. Bowers, *J. Am. Chem. Soc.* **2010**, *132*, 13486–13494.

[16] D. Drewes, E. M. Limanski, B. Krebs, *Dalton Trans.* **2004**, 2087–2091.

[17] A. Dolbecq, E. Dumas, C. R. Mayer, P. Mialane, *Chem. Rev.* **2010**, *110*, 6009–6048.

[18] A. Proust, R. Thouvenot, P. Gouzerh, *Chem. Commun.* **2008**, 1837–1852.

[19] B. Hasenknopf, R. Delmont, P. Herson, P. Gouzerh, *Eur. J. Inorg. Chem.* **2002**, 1081–1087.

[20] Crystal data and structure refinement for $[N(n\text{-}C_4H_9)_4]_3$-$[MnMo_6O_{18}(C_{13}H_{23}O_3)_2]\cdot(CH_3CN)_2$ (**1**): $C_{78}H_{146}MnMo_6N_7O_{24}$, $M_r = 2196.60$; orange block crystal, $0.54 \times 0.25 \times 0.11$ mm^3; $T = 150(2)$ K; monoclinic, space group $C2/c$, $a = 30.7603(9)$, $b = 50.8895(11)$, $c = 28.2617(7)$ Å, $\beta = 121.056(1)°$ $V = 37898.9(17)$ Å^3, $Z = 16$, $\rho = 1.540$ g cm^{-3}, $\mu(Cu_{K\alpha}) = 7.929$ mm^{-1}, F(000) = 18112, 133628 reflections measured, of which 33782 are independent ($R_{int} = 0.0770$), 1991 refined parameters, $R_1 = 0.0927$, $wR_2 = 0.2191$ (all data). $[N(n\text{-}C_4H_9)_4]_3$-$[MnMo_6O_{18}(C_{18}H_{34}NO_4)_2]\cdot((CH_3)_2NCHO)_4$ (**5**): $C_{96}H_{204}MnMo_6N_9O_{30}$, $M_r = 2595.26$; colorless, block crystal, $0.44 \times 0.24 \times 0.16$ mm^3; $T = 150(2)$ K; monoclinic, space group $C2/c$, $a = 49.3644(10)$, $b = 28.2598(5)$, $c = 25.5045(4)$ Å, $\beta = 99.785(2)°$ $V = 35061.9(11)$ Å^3, $Z = 12$, $\rho = 1.475$ g cm^{-3}, μ-$(Cu_{K\alpha}) = 6.559$ mm^{-1}, F(000) = 16320, 75954 reflections measured, of which 26802 are independent ($R_{int} = 0.1231$), 1181 refined parameters, $R_1 = 0.0972$, $wR_2 = 0.2667$ (all data). Crystal data were measured on a Gemini Oxford diffractometer using $Cu_{K\alpha}$ radiation ($\lambda = 1.54184$ Å) at 150(2) K. CCDC 819994 (**1**) and CCDC 819995 (**5**) contain the supplementary crystallographic data for this paper. These data can be obtained free of charge from the Fachinformationszentrum Karlsruhe, 76344 Eggenstein-Leopoldshafen, Germany (fax: (+49) 7247-808-666; e-mail: crysdata@fiz-karlsruhe.de).

[21] J. Zhang, Y. F. Song, L. Cronin, T. Liu, *Chem. Eur. J.* **2010**, *16*, 11320–11324.

[22] C. P. Pradeep, M. F. Misdrahi, F.-Y. Li, J. Zhang, L. Xu, D.-L. Long, T. Liu, L. Cronin, *Angew. Chem.* **2009**, *121*, 8459–8463; *Angew. Chem. Int. Ed.* **2009**, *48*, 8309–8313.

[23] J. Ling, C. M. Wallace, J. E. S. Szymanowski, P. C. Burns, *Angew. Chem. Int. Ed.* **2010**, *49*, 7271–7273.